Article

Damage Detection in Fiber-Reinforced Foamed Urethane Composite Railway Bearers Using Acoustic Emissions

Pasakorn Sengsri [1] [iD]**, Chayut Ngamkhanong** [1] [iD]**, Andre Luis Oliveira de Melo** [1]**, Mayorkinos Papaelias** [2] **and Sakdirat Kaewunruen** [1,*] [iD]

[1] Laboratory for Track Engineering and Operations for Future Uncertainties (TOFU Lab), School of Engineering, The University of Birmingham, Edgbaston B15 2TT, Birmingham, UK; pxs905@student.bham.ac.uk (P.S.); cxn649@student.bham.ac.uk (C.N.); alo888@student.bham.ac.uk (A.L.O.d.M.)

[2] School of Metallurgy and Materials, The University of Birmingham, Edgbaston B15 2TT, Birmingham, UK; m.papaelias@bham.ac.uk

* Correspondence: s.kaewunruen@bham.ac.uk

check for updates

Abstract: To a certain degree, composite railway sleepers and bearers have been recently employed as a replacement for conventional timber sleepers. Importantly, attributed to the rise in traffic demand, structural health monitoring of track structural members is essential to improve the maintenance regime and reduce risks imposed by any structural damage. A potential modern technique for detecting damage in railway components by using energy waves is called acoustic emission (AE). This technique has been widely used for concrete structures in other engineering applications, but the application for composites is relatively limited. Recently, fiber-reinforced foamed urethane (FFU) composites have been utilized as railway sleepers and bearers for applications in the railway industry. Neither does a design standard exist, nor have the inspection and monitoring criteria been properly established. In this study, three-point bending tests were performed together with using the AE method to detect crack growth in FFU composite beams. The ultimate state behaviors are considered to obtain the failure modes. This paper is thus the world's first to focus on damage detection approaches for FFU composite beams using AE technology, additionally identifying the load-deflection curves of the beams. According to the experimental results, it is apparent that the failure modes of FFU composite beams are likely to be in brittle modes. Through finite element method, the results were in good agreement with less than 0.14% discrepancy between the experimental and numerical data. The attractive insights into an alternative technique for damage assessment of the composite components will help railway engineers to establish structural monitoring guidelines for railway composite sleepers and bearers.

Keywords: railway sleepers and bearers; acoustic emission (AE); Fiber-reinforced Foamed Urethane (FFU); composite structures

1. Introduction

To date, the railway industry has embarked on the adoption of composite materials for rail infrastructures. Recent developments aim for the applications of composite materials to either rolling stock or infrastructure components such as train bogies, train bodies, railway sleepers and bearers, and so on. The general materials employed to fabricate railway sleepers and bearers are timber, concrete, and steel with 20, 50, and 50-year design life, respectively [1]. Over almost 200 years, timber sleepers and bearers have been used in railway tracks around the world, and they are aged and

need to be replaced. A main benefit of these wooden sleepers and bearers is their flexibility, which results in an excellent ability to withstand vibrations induced by dynamic loads in the railway track system [1]. On the other hand, the demand for other materials has grown because of a scarcity of good quality timber, expensive cost, and more maintenance needs. At the same time, concrete and steel sleepers and bearers have emerged as choices for new tracks; their size and structural integrity commonly limit their use to positions where successful sleeper/bearer replacement is undertaken [2]. Thus, new wooden sleepers and bearers remain a more favorable alternative in a short term to replace the deteriorated sleepers and bearers in areas consisting of maintenance of existing timber tracks, turnout sleepers and bearers (switch ties), and transoms (bridge ties) [2]. Additionally, their improved life cycle is significantly beneficial to these areas, which are very difficult to maintain. Another benefit of employing these sleepers is to be able to handle the constant increase in concern throughout the existing environment in the present industry because of its sustainable method.

Recently, reinforced polymer sleepers and bearers have become a potential alternative to timber sleepers and bearers. Compared to concrete and steel, reinforced polymers can be designed to mimic timber behavior, require nearly no maintenance, and are more sustainable from an environmental perspective. However, the cost is still approximately 5–10 times higher than that of a standard timber sleepers and bearers, making them commercially unviable [2]. In Australia, there have been two different types of polymer sleepers and bearers (polymer sleepers with short or no glass fibers and with long longitudinal glass fiber reinforcement) used in railway systems, and they have been available in the market for some time. Over the past 40 years, fiber-reinforced foamed urethane (FFU) composites have been applied to railway track system as sleepers or bearers to replace the conventional ageing timber sleepers and bearers. Due to the time-dependent capacity of timber components, it is important to develop polymer and composite sleepers that have a longer service life and can replace the old timber sleepers. FFU sleepers and bearers are reinforced with long continuous glass fiber reinforcements in the longitudinal direction. The longitudinal shear strength and stiffness is mainly controlled by long glass fibers, whilst it is dominated by polymers in the lateral direction [3]. The sleepers and bearers are suitable for ballasted rail tracks where stresses in them are controlled by bending loading, but less than ideal in special areas (i.e., turnout systems, transoms), where these sleepers and bearers are subjected to a high degree of combined flexural and shear forces as well as impact loading [3]. Moreover, FFU sleepers and bearers have superior properties to standard timber ones, for example, light weight; good resistance to water absorption, heat, and corrosion; easy drill ability; and more than 50 years of design life [3]. In the other words, a key challenge for railway engineers is to deal with low shear strength and shear modulus, limited design flexibility, low fire resistance, and high cost of FFU sleepers and bearers [3]. In terms of occupational health and safety during installation of FFU sleepers and bearers, we strongly suggest that personal protective equipment (PPE) for environmental health be required during on-site drilling of FFU sleepers and bearers in railway tracks. This is because small glass fibers can reach the lower part of the lungs, resulting in the increased risk of adverse health effects.

In practice, railway sleepers and bearers are some of the most critical structural elements in railway track infrastructures. The key functions of railway sleepers and bearers are to support the rails and to redistribute trainloads to the underlying layers [4]. They also help to ascertain safe rail gauge that permits trains to travel securely [5–7]. Thus, their structural behavior and performance over their entire service life are critical to assure public safety [8–11]. It is important to note that a railway track can be degraded over time, resulting in poorer track performance. Hence, it is very necessary to monitor and inspect their conditions, in order to prioritize and plan effectively the maintenance regime. The use of non-destructive technologies (NDTs) for such an inspection is still very limited due to the lack of insight into the structural performance with respect to a monitoring system. However, a significant increase in operational demand (e.g., to operate trains more frequently and more hours) has restricted the ability for visual inspections. The requirement for an adequate monitoring system of railway sleepers and bearers cannot be neglected. In fact, the combination of NDTs and the advancement of "smarter tracks" can potentially attenuate the risk imposed by any damage to structural components. Railway

engineers would gain the benefits of the developed smarter tracks (via the installation of sensors and real-time condition monitoring system) for future maintenance activities and railway services [12,13].

Presently, common damage detection techniques, in addition to visual observation, are unsuccessful to identify any component damage in real-time, and they cannot perform to completely reduce track possessions. Interestingly, acoustic emission technology has been extensively used in numerous engineering applications to detect crack growth, remaining life, source of damage, and fatigue life of structural members. Therefore, there is a high potential that AE application for railway composite beams can be realized. The AE function can collect real-time damage data and eliminate the drawbacks of the conventional methods of NDTs, leading to more secured railway tracks as well as minimizing long-term maintenance costs.

Based on previous literature, the behaviors of composite structures used in the railway industry have not been fully investigated. It is important to note that the industry frequently hesitates to adopt new composites, because of lack of a historical track record and adequate practical experience. Since standard testing methods are not sufficient to replace an element design approach, a certain monitoring and design approach requires future track maintenance that has adequately correct details about the exact service life of the structural and safety-critical element for harmful effects on rail environments. Recently, there have been numerous tasks to improve railway track performance so that railway tracks could be designed up to 50 years with conventional routine maintenance. Nevertheless, most of the railway sleepers and bearers could have pre-mature failure because of irregularities. Accordingly, the requirement of turnout bearers is to replace and adapt properly structural design and monitoring networks, in order to ensure the safety limit and structural reliability, which can be maintained with long term sustainability [14–16]. This paper identifies the potential of AE sensing for the evaluation of the responses of FFU composite beams. Three-point bending tests were carried out in order to use AE sensing techniques to detect the real-time crack growth. The failure modes and load-deflection curves of FFU beams were also identified. The insight of this study will provide significant engineering guidelines and assessments for structural health monitoring of FFU composite sleepers and bearers in public use.

2. Materials and Methods

2.1. Fiber-Reinforced Foamed Urethane Material

Fiber-reinforced foamed urethane (FFU) material for railway applications has been developed by SEKISUI Chemical Gmbh [17]. The FFU composite is an advanced material inspired by timber, which was first produced by Sekisui in 1978. Recently, the FFU composite material has been extensively utilized in Japan's railway infrastructures, from high-speed Shinkansen to regional trains and urban subway networks. Over decades, FFU sleepers have been installed in more than 870 km of railway tracks, and the primary areas of applications are at railway switches and crossings and transom bridges. According to Gunther [18], earlier studies identified that wood sleepers (which are made of at least 70 percent of original wood content) are vulnerable to be damaged due to aggressive loadings and to be eroded due to the weather conditions. As a result, these concerns have led to intensive research for advanced materials to compensate for the weak performance of the wooden sleepers and to recover the advantages of the wooden sleepers (such as damping and constructability). The properties of FFU synthetic material are tuned to be nearly equal to those of native timber materials.

However, it is noted that the service life of FFU material is much longer than that of native timber materials, and the weathering resistance is even better. The FFU composites are easier to be produced and the resources of composites are widely available. The FFU material has higher electrical insulation in both wet and dry conditions and can be mass-produced. In 1996, various static and dynamic investigations on first synthetic sleepers from the experimental track sections were carried out by Railway Technical Research Institute (RTRI). The lifecycle of the FFU sleeper is predicted to be over 50 years, depending on the outcomes collected at the time [18]. Furthermore, once the Technical

University of Munich showed that the FFU composite sleepers effectively behave under fatigue loadings, this test aimed to highlight the superior redistribution of plastic displacement occurred by high trackpad forces, sleeper screw pulling forces, and derailment impact loadings. The FFU material is much more enduring than a native wood material. Takai et al. [19] pointed out the durability based on the use of Japanese FFU sleepers for more than 15 years, mainly for the open plain tracks and for a transom bridge. The result showed that after 15 years of use, the short sleepers had no cracks or damage on the surface, and had no flexural deformation on the whole component. The whole color and size of the FFU composite sleepers were stable.

2.2. Acoustic Emission Sensing

In 1950, many early types of research utilizing AE were conducted, and various concepts leading to its most effective application, whether industrially or commercially came about. There was immediate development in the technology in later decades, and by the 1970s it was an important approach of structural monitoring. Acoustic emission (AE) defines the production of transient elastic waves by an immediate redistribution of stress in a material. When a structure is imposed to external forces, also known as an external stimulus (change in temperature, force, or pressure), local sources release the stress waves to the surface of a material, and they are recorded by devices or sensors [20], as demonstrated in Figure 1. Basically, crack initiation and propagation, which appear in FFU railway sleepers, is the stress sources, for example, when the loading of rolling stock is applied to a sleeper, influencing crack propagation, and then a signal is released from the tip of the crack identifying its position and growth rate. The AE waves are likely to be interfaced by a passing train, which generates disturbances called extraneous noise [20]. This noise is detectable by its clearly noticeable frequency spectra; thus, it is able to be found for the important AE waves [21]. Furthermore, current technology deals with this problem by utilizing the master–slave method. This means using "guard sensors" to eradicate extraneous noise [22].
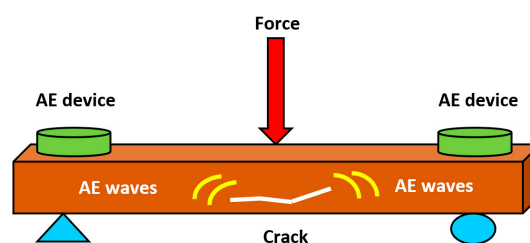

Figure 1. Acoustic emission (AE) technique.

Accordingly, the acoustic emission technique (AET) has been generally utilized for damage detection of structures and real-time data collection. Compared to other non-destructive testing (NDT) techniques, there are two important differences between AET and NDT. The first key is that AET produces its own signal. For another difference, AET is often used to detect movement on structures during operation, whilst most other conventional techniques determine existing geometrical discontinuities. However, the AE method can only qualitatively measure how much damage is carried in a structure. A further disadvantage of AE is that it gives intense noise signals.

2.2.1. Application of AE Sensors

One of the most useful situations of using AE sensing is long-term observation. Once the AE technology has been placed it can be left to perform structural health monitoring without physical maintenance. Therefore, this possible method is helpful to identify the damages. In the last 40 years, a structural health monitoring technique was used for determining the locations of fiber breaks, in order to identify the actual distribution of fiber fragments, when a load was applied to a composite sample consisting of a single fiber to analyze the failure test [23]. After this, the shear strength of

the fiber–matrix interface was identified by the micro-mechanical simulation from the measurement of fragmentation lengths [23]. Another instance of using the acoustic emission (AE) approach is for concrete engineering. This approach is able to monitor concrete structures in practice and also to evaluate the damage level of structures. According to Masayasu [24], a standard referred to as the AE Kaiser phenomenon in the suggested practice has been now set by the Japan Non-destructive Testing Association. Damaged qualifications define the ratio relationship between the load and calm of the new AE parameter [24]. Additionally, this led to investigating the possibility of damage detection in reinforced concrete beams under incrementally repeated loading. The outcomes indicate that the two types of qualified damages are certain with the real damages of the beam [25]. A third example of this might be, in 2012, the task of repair for the Hammersmith flyover in London, which utilized more than 400 AE sensors in order to detect tendon failure [26].

The AE system was not only completely efficient. This is because the AE devices were placed for long periods of time after the initial construction; thus, the already defected structure was taken as the base condition [27]. For a railway application, implementation on tracks would have the identical flaw, as damage to the sleepers may only be detected during installation, even if the structure had already failed. Nevertheless, the data remains useful as the sleepers with the most propagating cracks can be identified. In a further example of using the AE technique, A Clark et al. [28] conducted an experiment using the AE method to determine damage in railway prestressed concrete sleepers. It was found that this method could give precise data, exactly detecting the position and range of sleeper damage. Obviously, it provides a successfully fundamental criterion for material damage and service life. It is of extreme importance for timely maintenance of elements and secure operation of structures to prevent unpredictable incidents. As a result of these cases, applications on railway structures are likely to have the identical imperfection, as damage to the sleeper may be particularly detected during the installation. Nevertheless, the data collections remain useful as the sleepers with the most continuous cracking can be determined.

2.2.2. Kaiser Effect

AE signals produced under various loading patterns can provide useful information in terms of the structural integrity of a material. The possible AE signals could be identified when the previous loading has been suddenly surpassed. The increase in rate is known as the Kaiser peak, and this phenomenon is known as the Kaiser effect. Later, the extend of the research was not restricted to metallic materials. This led to many researchers investigating studies of acoustic emission techniques for concrete damage detection. The results indicate that the Kaiser effect is acceptable for experiments on concrete engineering [29]. Holcomb [30] stated that in 1950, Kaiser was the first German who researched AE technology in training. Furthermore, Joseph Kaiser mentioned that a material almost generates no identified emission signals until the prior highest stress degree is gained, under elastic behavior [31]. Hence, the Kaiser effect is very significant for repeated loads of railway systems. Other studies have also shown that a repeated load would not impact the acoustic emission outcomes until the previous highest stress degree was carried out [31].

2.3. Methodology

2.3.1. Three Point Bending Test

Based on EN 13230-2 bending testing [32], it requires positive and negative bending tests for sleepers at the rail seat support. Only positive bending tests were achieved due to the symmetrical shape of the specimens. This means that the samples have the same positive and negative capacity. The setup of the three-point bending test is shown in Figure 2. The criterion needs articulated support and must be 100 mm wide, made of steel with Brinell:HBW > 240. A static load was applied at the mid-span to conduct a 3-point bending test. Note that the three-point bending behavior will excite the center-bound issues connected to poorly maintained ballast beds. When the railway beam

does not distribute forces into the ballast, it will produce negative bending behavior to the structure. The positions of sensors had been strategically installed to detect the position criticality of the AE sensors and to assess the sensing wave simplicity (Figure 3). Three AE devices were utilized in each test, and a linear variable differential transformer (LDVT) was placed at the mid-span position of the specimen to obtain the deflection. Four strain gauges were located at the front and rear locations of the individual specimens to record stress variations. Figure 4 demonstrates two pattern tests of the samples under two different loading conditions. The investigations were sufficiently performed in order to comply with the BS EN 13230-1 standard [32]. As for a single load test, the FFU beam specimen was loaded until failure. Another specimen for the repeated load test was loaded until the first crack appeared. The first crack load was measured, and the specimen was then unloaded. This specimen was reloaded and unloaded again until it reached 1.5 and 2.5 times the load corresponding to the first crack so that there were three loading cycles in this test. Lastly, the ultimate load was applied to observe the failure mode of FFU beam.

Figure 2. Testing arrangement of a full-scale test.
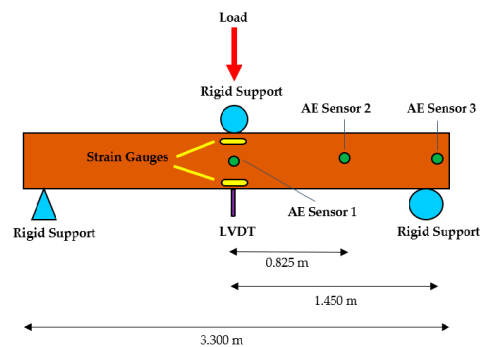
Figure 3. Schematic view of the linear variable differential transformer (LVDT) and the sensors used.
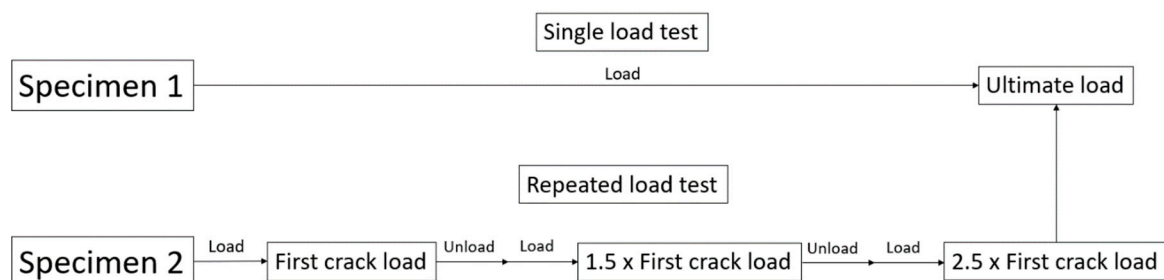

Figure 4. Testing procedure of the single load test and the repeated load test.

2.3.2. AE Equipment

AE measurement was achieved throughout the mechanical experiments of all the sample types to monitor and assess damage growth under bending loading. The AE waves were identified and collected utilizing a 4-channel DAQ AE network generated from Physical Acoustic Corporation (PAC, now Mistras). The data acquisition was conducted using "AE-Win" software. The AE waves were determined employing wideband PAC-WD piezoelectric acoustic transducers performing at a frequency range of 20 to 1000 kHz. The data acquisition network used was a custom-built AE and vibration acquisition network able to continuously record the full waveform for periods of a few seconds. The custom-built acquisition network was comprised of the following parts:

- A computer with a customized data logging program.
- An Agilent U2531A 4 channel data acquisition card.
- A 4-channel decoupling hub.
- MISTRAS wide bandwidth AE amplifier given by PAC.
- A PAC model 2/4/6 preamplifier operating with a range of frequency from 20 to 1200 kHz.
- A wideband PAC-WD piezoelectric AE sensor operating with a range of frequency from 20 to 1000 kHz.

3. Experimental Results

3.1. Crack Propagation and Failure Mode

Under the load increment, damage and crack propagation were marked and recorded. As for the first sample, the first crack (fracture of internal fibers) under a single load test appeared at 34 kN and failed at 132 kN. The fiber cracks could be observed longitudinally along the fiber orientation (Figures 5 and 6). Additionally, the substantial crack exceeded 25 mm in width. The sudden rupture could be seen through the delamination of fibers along with the beams. As for the second sample subjected to repeated load, it was found that the first cracks were observed at 67 kN. The sample was reloaded until it reached 1.5 of the first crack load resulting in more cracks that could be seen. However, the beam still behaved in a linear elastic range, as seen in Figure 6. The sample was then reloaded again until 2.5 times the first crack load. It was clearly seen that the behavior was in the minor plastic range, and permanent deformation was observed. The sample completely failed under the load of 170 kN, where a mix of tensile and splitting cracks could be seen (Figures 5 and 6). As shown in the crack patterns, it was clear that the FFU beams were likely to have brittle failure modes.
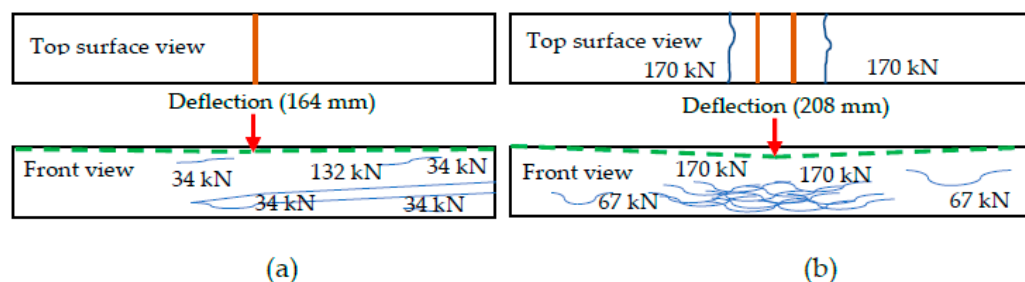

Figure 5. Damage behaviors of full-scale fiber-reinforced foamed urethane (FFU) composite beams under (**a**) single load test at 132 kN; (**b**) repeated load test at ultimate load (170 kN).
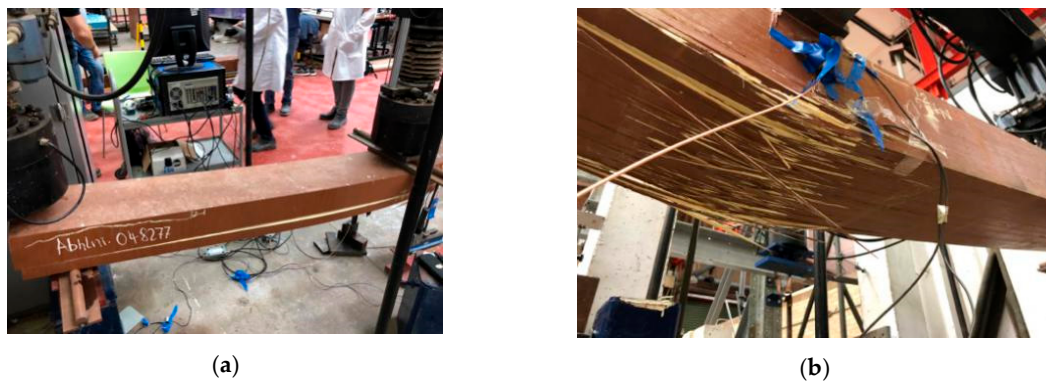
(**a**)   (**b**)

Figure 6. Failure mode of full-scale FFU composite beams under (**a**) single ultimate load; (**b**) repeated load.

3.2. Acoustic Emission (AE) Signals

The load–deflection curve shows the elastic and plastic behavior under three-point bending tests with the linear portion showing the elastic area and the nonlinear curve indicating the plastic zone. The load–deflection curves together with AE signals can be found in Figures 7 and 8. The data was collected by the AE devices and it completely detected the damage in the FFU composite beam under the single load test. The highest energy was predicted to appear at the period of ultimate damage, and the beam still had tensile capacity. However, the recording series of the linear variable differential transformer (LVDT) was not adequate to collect the data due to large deflection in the next activity. Thus, it was replaced to use a scale recording, which would create some changes. However, it would not influence the whole test.

Figure 7 demonstrates the incremental loading arrangement from the damage progression test (under single load test). Compared to the failure curve, the energy hits were not extremely high. On the other hand, it was clear that the initial cracking could be observed at 34 kN, as shown in Figure 5. In addition, all the initial energy occurred at the middle sensor, which was nearest the cracking source, and there were no signals from the other two sensors. Before the initial damage occurred, an AE activity corresponded to slight internal damage, fiber cracks, and extraneous noise. This was because, due the Kaiser phenomenon when the beam was unloaded and reloaded back to the loading needed for the initial crack, there was no AE activity, and hence it was likely to put these in a single time sequence. In fact, the damage changed the flexibility of the beam. Therefore, this was a reason why for 1 mm deflection, the load could be less than 2 kN. Moreover, the maximum deflection was 164 mm at the ultimate load of the sample, around 132 kN.
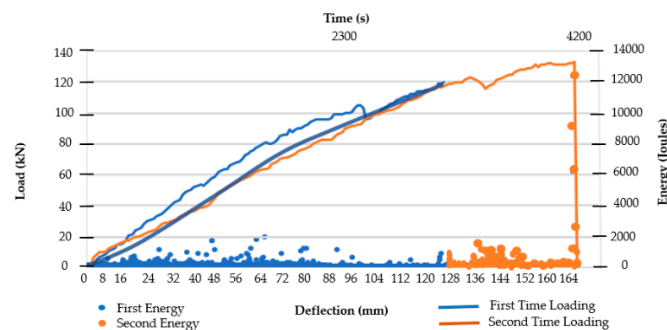

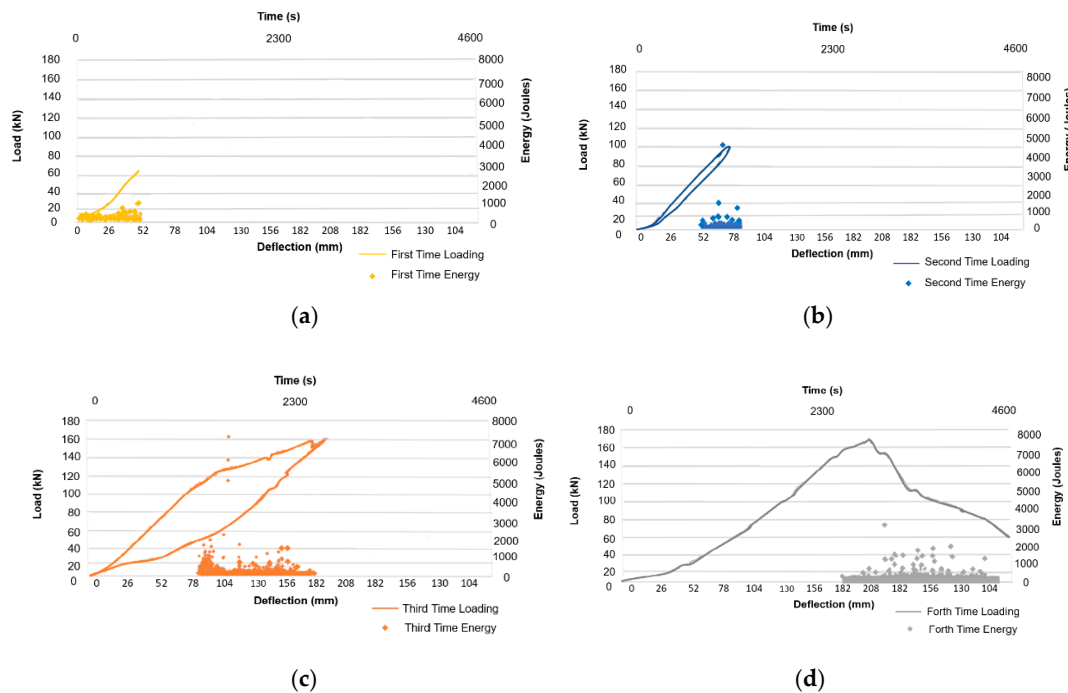**Figure 7.** Load–deflection against AE energy under single load test.

Figure 8. Load–deflection against AE energy under repeated load: (**a**) fist crack load; (**b**) 1.5 times the first crack load; (**c**) 2.5 times the first crack load; (**d**) ultimate load (170 kN).

Figure 8 illustrates the incremental loading arrangement from the crack progression test (under repeated load test). It confirmed that when the first damage occurred at 67 kN, the sample continued to be damaged, but these damages or fiber cracks were not obvious. Whilst energy from the first damage event was insignificant, as shown in Figure 8a, therefore it could not be observed because of the Kaiser phenomena. When the beam was reloaded to 100 kN, the maximum energy signal of the second time loading was 4500 joules, as presented in Figure 8b, which exhibited that internal cracks had begun to occur significantly. The maximum energy signal of 7500 joules appeared at the third time loading, as given in Figure 8c, and the maximum deflection of 208 mm took place at the ultimate load of the sample, 170 kN, shown in Figure 8d. After this point, the vast cracks had appeared and at the same time abundant fiber had cracked. After the first damage, the slopes of the curves showed the transmission into the plastic area, where general AE activity was maintained. Contrasting the damage progression to the AE energy hits, there was a powerful correlation between the two energy hits, confirming the ability of employing AE in damage determination. As a result, there were obviously peaks and troughs in the energy sequence that illustrated any dominant cracking phenomena that were taking place.

Figures 9 and 10 display the micro-strains versus acoustic emission energy over time in compression and tension modes under the single load test, respectively. As seen in Figure 9a, the highest micro-strain of nearly 2300 μm/m took place at the ultimate load of the sample in compression failure mode, whilst in tension failure mode it reached 5500 μm/m in Figure 10a. The line segments in the two figures marked by the red lines had no signal record because the damage had destroyed the strain gauge sensors, which were later reconnected. The yellow arrows in the diagrams show the reloading again. The graph of micro-strain compression mode was uncommon because the chips in the gauges were placed near the support position. When the force was reloaded, the initial point of strain did not begin from zero, which expressed that the material had previously experienced insignificant deformation. Comparing to tension mode, acoustic emission data could provide its correlation. When unloading occurred again, the tensile strength was likely to be zero. This meant the high tensile strength and the maximum energy in the final stage exceeded 14,000 joules. There were also no subsequent records due to the material and strain gauges being destroyed.
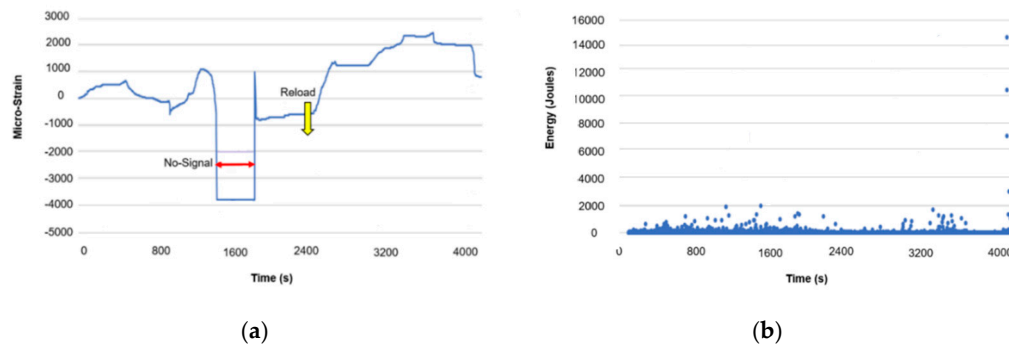
Figure 9. Micro-strain and AE energy over time in compression mode under single load test (**a**) micro-strain; (**b**) AE energy.
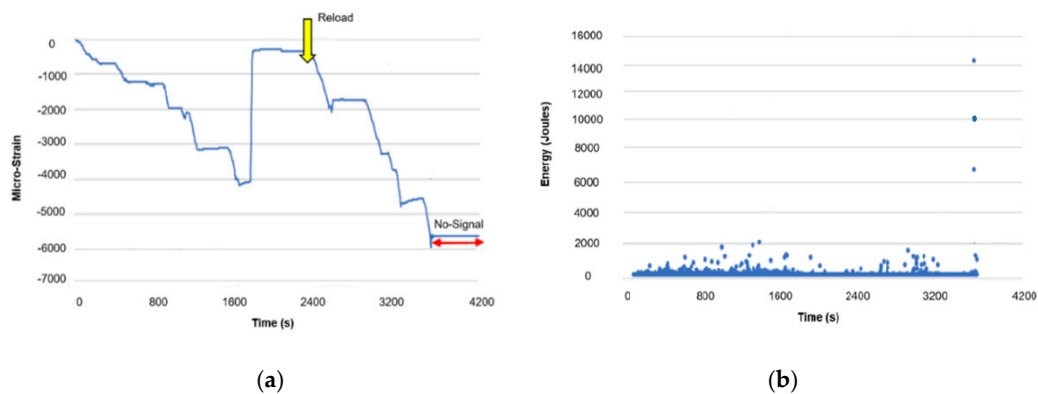

Figure 10. Micro-strain and AE energy over time in tension mode under single load test (**a**) micro-strain; (**b**) AE energy.

Figures 11 and 12 show the micro-strains versus acoustic emission energy over time in compression and tension modes under repeated load test, respectively. In Figure 11b, it can be seen that there were some vacant energy areas due to the Kaiser effect. The highest energy and strain compression mode under repeated load test occurred in the first phase (first time loading) with no more than 1500 joules and 1500 μm/m, respectively. It was noted that the calibration recorder could collect up to 30 mm per time, and it was thus essential to manually adjust the calibration recorder without interrupting the experiment to take place at the calibration zero phase.
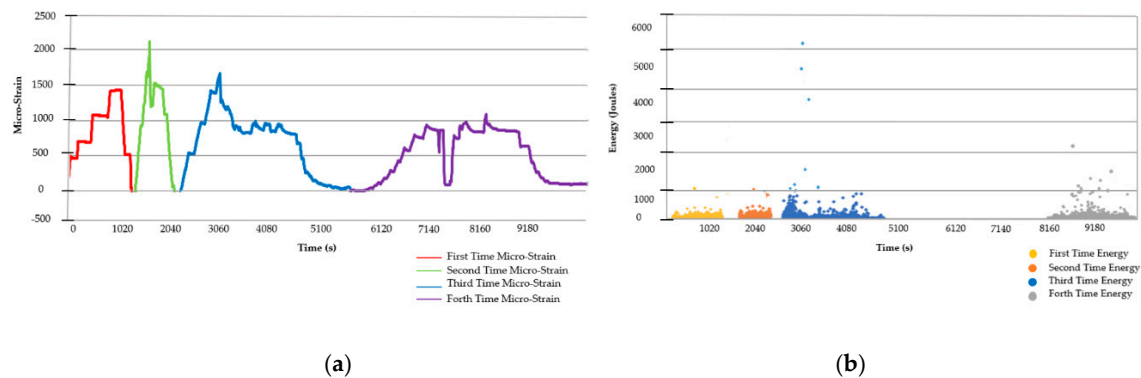

Figure 11. Micro-strain and AE energy over time in compression mode under repeated load test (**a**) micro-strain; (**b**) AE energy.
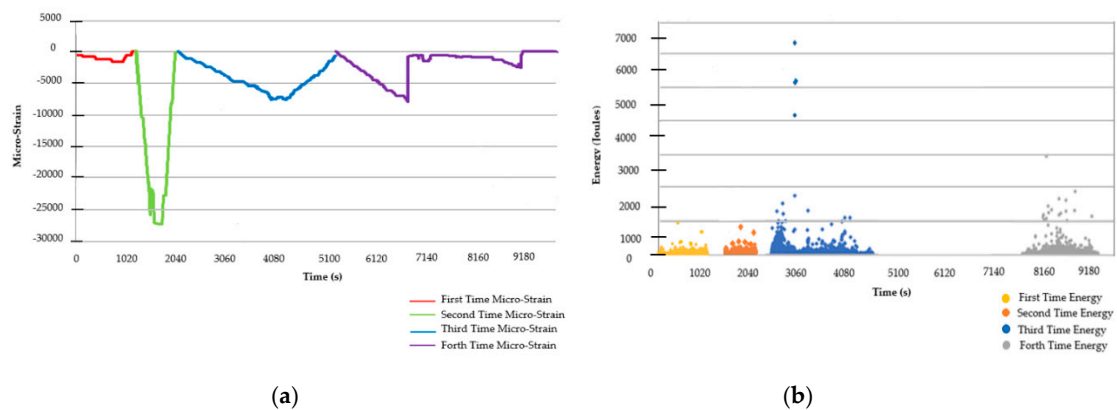
(**a**)　　　　　　　　　　　　　　　　　　(**b**)

Figure 12. Micro-strain and AE energy over time in tension mode under repeated load test (**a**) micro-strain; (**b**) AE energy.

The highest energy signal in the second phase of the graph in compression mode was still 1500 joules when compared to the previous phase, whilst the maximum micro-strain was 2200 μm/m in compression mode. Nevertheless, there were two unclear cracks on the top surface of the material. When the third reloading reached 167 kN, the highest energy signal was more than 5500 μm/m and also the micro-strain repeatedly reached almost 1700 μm/m. This was because of the limit of the length of the hydraulic column press; thus, the experimental tools had to be unloaded and reloaded for the fourth time. The AE wave repeatedly appeared after the force exceeded 167 kN. Another AE activity appeared before the previous AE signal, due to the effect of external noise, but it could be ignored. However, when the force reached the ultimate load (170 kN), many fractures occurred at the lowest part of the sample, nearly damaging a third of the zone, and some fibers were eliminated. The two maximum values of micro-strain in the latter two phases were lower than those in the previous two phases, which presented that the material properties had changed.

As illustrated in Figure 12, it was obvious that the micro-strains and the energy hits were relatively low in the first stage of damage until the load exceeded 67 kN. Then, the energy rose sharply, and the peak value of micro-strain was more than 25,000 μm/m. It was noted that the corresponding energy hits were relatively low when there were no serious damage or cracks in the component. This meant that the materials of the beam had very high tensile strength. In the third stage, the maximum micro-strain was more than 7000 μm/m, which was less than the previous maximum value in the second stage. Additionally, the maximum energy in the third phase was more than 6000 joules, and it was evident that the highest energy occurred when the largest cracks appeared in the beam at the nearly ultimate load condition. It was found that the micro-strain value was low because the component reached the failure condition. This caused the strain gauge to fail to record the data.

4. Numerical Analysis and Results

4.1. Classical Beam Theory

Currently, structural engineers attempt to estimate the deflections of a beam under flexural loading, and there are some theories to determine the beam deflections, depending on the assumptions of their theories [33–36]. One of the most extensively adopted beam theory is the Euler–Bernoulli beam theory, also known as classical beam theory. The two elementary assumptions of this theory are that the deflections are still small and the cross-sections of the beam under deflection are still perpendicular to the deflected axis (i.e., elastic curve).

In terms of a simple beam under a mid-span load point, the equation of bending moment equation of the beam to determine the maximum bending moment can commonly be represented by

$$M_{max} = \frac{PL}{4},$$

(1)

where M_{max} is the maximum bending moment (Nm), P is the load point at mid-span of the beam (N), and L is the full length of the beam measured between centers of support (m). As is known, the maximum deflection of a simply supported beam appears at the mid-point. Hence, the equation of the maximum deflections can be identified by

$$\delta_{max} = \frac{PL^3}{48EI},$$ (2)

Herein, δ_{max} is the maximum deflections at the centre (m), E denotes the elastic modulus of the material from that the beam is manufactured (N/m^2), and I expresses the area moment of inertia (m^4).

4.2. A Finite Element Model of the FFU Composite Beam

According to our previous work in [4], the numerical investigation of flexural behavior of a composite beam (using FFU material) acting as a bearer in a railway system was performed. Several studies showed how three-dimensional finite element models of concrete sleepers could be developed and investigated for railway track elements [37–46], but there are nearly no studies on composite railway sleepers and bearers. In this simulation, the composite (FFU) material components were modeled as a three-dimensional finite element model of a FFU composite beam based on Euler–Bernoulli beam theory. The 2D beam elements were adopted for the model because the experimental results suggest that the composite bearers behave like a shallow elastic beam in accordance with Euler–Bernoulli theory. The simple beam model was composed of 24 beam elements with 49 nodes using LS-DYNA software [47], given in Figure 13. The load of 170 kN (ultimate load) was applied to the mid-span. Table 1 indicates the engineering properties of the model used in this simulation. The values of these properties were selected due to the similarity of a special type of a bearer fabricated in the UK. This section aims to determine the load–deflection curve of a FFU composite beam in flexural mode under static loading. The potential quality of finite element method expressed a flexural behavior of the FFU composite beam, which was affected by the deflections and bending moments, as given in Figure 14, respectively. Clearly, the model could offer adequate evaluation of the beam's flexural behavior under static load when compared to the experiment tests in the following section. The validation of this numerical modelling was carried out in the last part.

Table 1. Engineering properties employed in the simulation model.

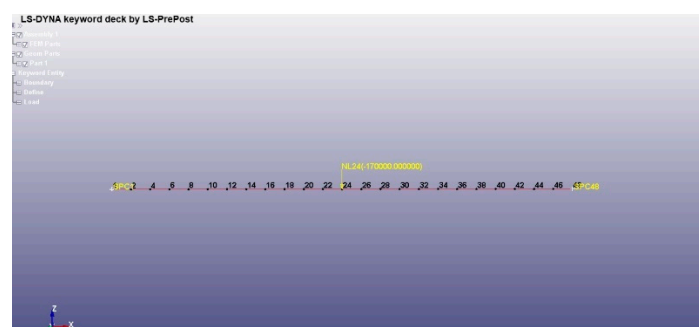| Parameter lists	Values	Units
Elastic modulus	8100	MPa
Poisson's ratio	0.25	-
Density	740	kg/m
Beam length	3.3	m
Rectangular cross-section (depth 0.16 m * width 0.26 m)	0.042	m^2

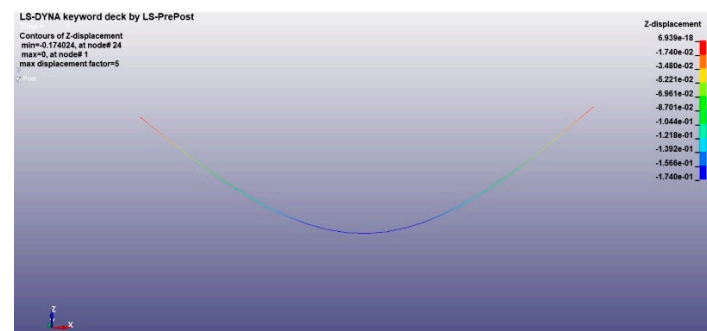**Figure 13.** Finite element simulation model of a simply supported FFU composite beam.

Figure 14. Finite element method for determining deflections of a FFU composite beam under bending loading.

4.3. Validation of the FFU Composite Simulation Model

To validate the numerical model of a FFU composite beam components acting as a bearer for switch or crossing areas in the railway system, the analytical solution based on classical beam theory was used. Since FFU absorbed very little energy before fracture and did not show a significant plastic zone according to the load–deflection curves, it is important to note that elastic properties were assumed in the model as the FFU was likely to be brittle. A comparison between the finite element method (FEM) and the analytical solutions is presented in Table 2. It was found that the results provided a percent error less than 2%. Therefore, it is likely to efficiently utilize analytical solutions to identify the maximum bending moment and deflection.
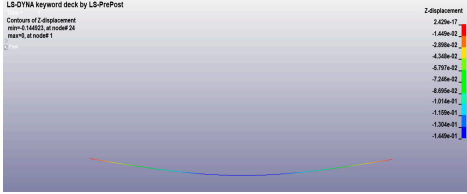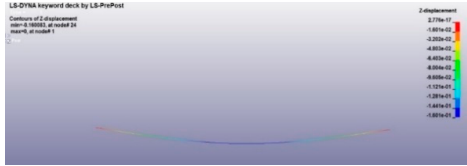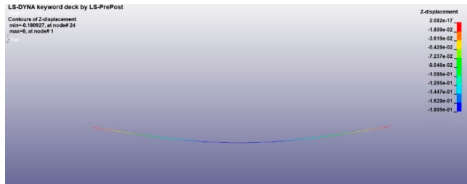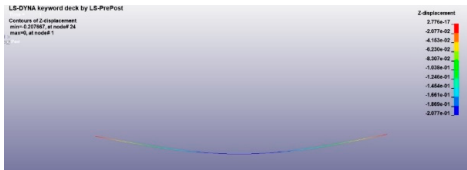
Table 2. Comparison of the FEM and the analytical solutions of the FFU composite beam under bending load.

	Theoretical	FEM	Error (%)
The maximum bending moment (kNm)	140.30	138.60	1.21
The maximum deflection (mm)	177.00	174.00	1.69

4.4. Determination of an Optimized Model for the FFU Composite Beam

To obtain an optimized model for the FFU composite beam, the finite element analysis used was carried out for estimating the elastic modulus and deflection of the beam under the single point load of 170 kN, which was compared to the experimental results. The maximum deflection of 208 mm was observed in the lab. In this simulation, the five different elastic moduli were used to determine the deflections of the models, as presented in Table 3. It is important to note that the values of elastic modulus properties in Table 3 were based on the dynamic elastic moduli extracted from our experimental measurements (i.e., natural frequencies). The slope of a curve showing a nonlinear relationship between different elastic moduli and deflections of the FFU composite beam models under bending load is depicted in Figure 15. It was found that a higher elastic modulus of the FFU composite beam under bending load yielded a lower deflection. As discussed, the FFU was found to be brittle, presenting a small plastic region before fracture, so that the nonlinearity was not taken into account. However, the nonlinear property should thus be considered in the near future once the stress–strain curves are obtained, as the finite element method (FEM) is capable of analysis of nonlinear complex composite materials. In this simulation, our main aim was to develop a realistic static model of railway tracks. Then, the model was used to predict its static responses to bending load for predictive and preventative maintenance to ensure railway safety. As static parameters from its responses, they are a significant factor to consider before fabricating a real structure to identify and tackle potential issues early in the design process. For load–deflection curves of the FFU composite beam models, it was discussed as given in the following part. The curve shows the difference between load–deflection curves obtained by numerical and experimental results.

Table 3. Finite element analysis for determining the optimized simulation model for a FFU composite beam under bending load.

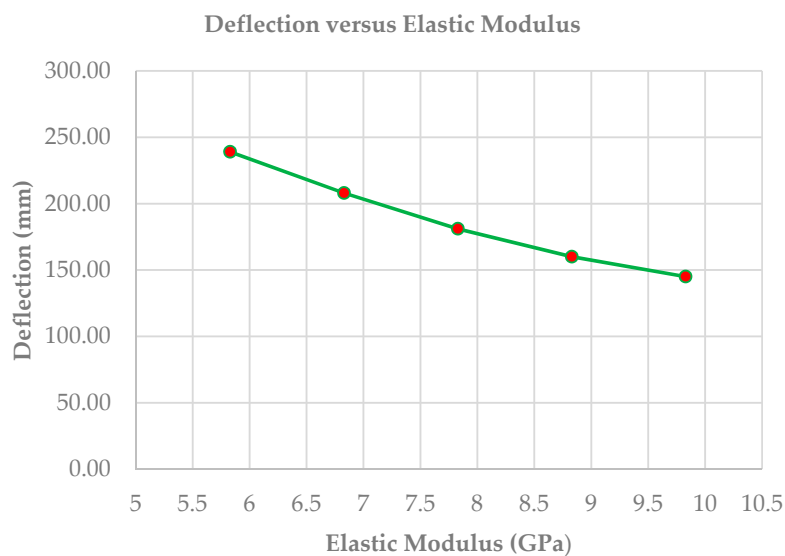| No. Models	Flexural Behaviors	Elastic Moduli, E (GPa)	Deflections (mm)	Difference (%)
1		9.83	144.90	30.34
2		8.83	160.10	23.03
3		7.83	180.90	13.03
4		6.83	207.70	0.14
5		5.83	239.30	−15.05

Figure 15. Relationship between elastic modulus and deflection of the FFU composite beam models under bending load.

5. Discussion

Based on experimental results, in both cases under single load test and repeated load test, it was found that the acoustic emission (AE) sensing technology was successful in the identification of initial crack activities. The energy hit occurred by these cracks correlated well with other parameters. AE activities were ineffective to anticipate at the end of the experiments when failure was likely to appear. Therefore, the failure mechanisms for these FFU composite beams should be repeatedly evaluated. Obviously, the data collected directly via AE identified the behavior of FFU composite beams under bending load. The experimental load–deflection curves provided a simple approach of real-time damage determination because vertical deformation recordings can detect changes in structural integrity. Furthermore, the load–deflection curves between the experimental and numerical data were found to be bi-linearly and linearly proportional, respectively. A comparison of the load–deflection curves with five different moduli of the FFU composite beam under bending load between the experimental and numerical data is presented in Figure 16. The results were in good agreement with less than 0.14% discrepancy when the elastic modulus of 6.83 GPa was chosen. Besides, the FFU beams behaved as elastic materials under static loading, based either on experimental or numerical results. It is important to note that the experimental load–deflection curves in Figure 8 tend to be bi-linear, whilst the load–deflection curves obtained from the numerical results in Figure 16 are likely to be linear. Therefore, the numerical elastic moduli extracted are secant moduli at an ultimate load of 170 kN.
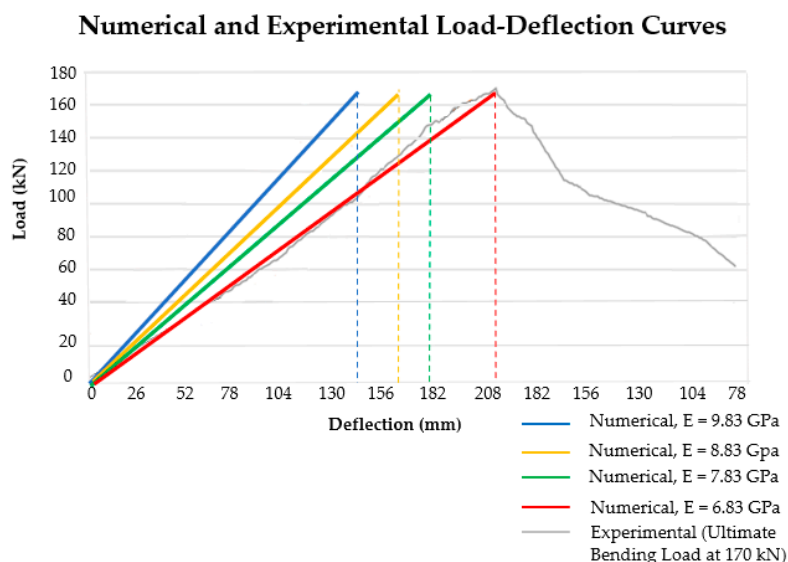

Figure 16. Comparison of the load–deflection curves between the numerical and experimental results under bending loading.

6. Conclusions

This study investigates an attractive damage detection approach for structural composite components used in railway switches and crossings using acoustic emission technique. Full-scale experiments were carried out to artificially create damage and failure following European standards. It is important to note that the acoustic emission technique was proven as an alternative method for structural damage detection. The experimental investigations into the acoustic emission method completely led to useful insights and findings for the structural health monitoring of the composite components. This paper is the world's first to investigate a damage detection method for FFU composite beams using acoustic emission technology, and to identify the load–deflection curves of the beams. Additionally, the study highlights the potential of self-monitoring systems by the AE technique, providing a positive case for their implementation on track structures. Surprisingly, the AE sensing results were successfully proven to enable effective detection of initial damage activities (i.e., fiberglass

snaps). The comparative results for the load–deflection curves were in good agreement with less than 0.14% discrepancy between the experimental and numerical data. These interesting insights will help railway engineers to effectively detect and monitor any damage in FFU composite beams, also developing realistic static sleeper/bearer models of railway tracks. Some findings from this study can be drawn as follows:

- FFU composite beams can fail in a brittle mode of failure.
- The rupture of FFU composite beams occurs rapidly through the delamination of fibers along the beams.
- There is no AE activity within FFU composite beams when the maximum loading does not exceed the previous loading, due to the Kaiser effect.
- The load–deflection curves of FFU composite beams are approximately bi-linearly proportional even if the structure is damaged.
- In this paper, the optimized FFU composite beam model has the elastic modulus E = 6.83 GPa when damages occur at the ultimate static load.

Author Contributions: Conceptualization, S.K. and M.P.; methodology, S.K.; software, S.K. and M.P.; validation, P.S., A.L.O.d.M., and C.N.; formal analysis, P.S., A.L.O.d.M., and C.N.; investigation, S.K., P.S., A.L.O.d.M., and C.N.; resources, S.K., M.P.; writing—original draft preparation, P.S.; writing—review and editing, S.K. and C.N.; visualization, P.S., and A.L.O.d.M.; supervision, S.K. and M.P.; project administration, S.K.; funding acquisition, S.K. All authors have read and agreed to the published version of the manuscript.

Conflicts of Interest: The authors declare no conflict of interest.

References

1. Ferdous, W.; Manalo, A.; Van, G.; Aravinthan, T. Evaluation of an Innovative Composite Railway Sleeper for a Narrow-Gauge Track under Static Load. *J. Compos. Constr.* **2018**, *22*, 04017050. [CrossRef]
2. Van Erp, G.; Mckay, M. Recent Australian Developments in Fibre Composite Railway Sleepers. *Electron. J. Struct. Eng.* **2013**, *13*, 62–66.
3. Ferdous, W.; Manalo, A.; Van Erp, G.; Aravinthan, T.; Kaewunruen, S.; Remennikov, A. Composite railway sleepers – Recent developments, challenges and future prospects. *Compos. Struct.* **2015**, *134*, 158–168. [CrossRef]
4. Kaewunruen, S.; Sengsri, P.; de Melo, A.L.O. Experimental and Numerical Investigations of Flexural Behaviour of Composite Bearers in Railway Switches and Crossings. In *Sustainable Issues in Transportation Engineering*; Mohammad, L., Abd El-Hakim, R., Eds.; GeoMEast 2019 Sustainable Civil Infrastructures; Springer: Cham, Switzerland, 2019.
5. Silva, É.A.; Pokropski, D.; You, R.; Kaewunruen, S. Comparison of structural design methods for railway composites and plastic sleepers and bearers. *Aust. J. Struct. Eng.* **2017**, *18*, 160–177. [CrossRef]
6. Kaewunruen, S. Discussion of "Evaluation of an Innovative Composite Railway Sleeper for a Narrow-Gauge Track under Static Load" by Wahid Ferdous, Allan Manalo, Gerard Van Erp, Thiru Aravinthan, and Kazem Ghabraie. *J. Compos. Constr.* **2019**, *23*, 07018001. [CrossRef]
7. Kaewunruen, S.; Remennikov, A.M.; Murray, M.H. Introducing a new limit states design concept to railway concrete sleepers: An Australian experience. *Front. Mater.* **2014**, *1*. [CrossRef]
8. Remennikov, A.M.; Kaewunruen, S. A review of loading conditions for railway track structures due to train and track vertical interaction. *Struct. Control Health Monit.* **2008**, *15*, 207–234. [CrossRef]
9. Remennikov, A.; Kaewunruen, S. Experimental Investigation on Dynamic Railway Sleeper/Ballast Interaction. *Exp. Mech.* **2006**, *46*, 57–66. [CrossRef]

10. Kaewunruen, S.; Remennikov, A.M. Application of vibration measurements and finite element model updating for structural health monitoring of ballasted railtrack sleepers with voids and pockets. In *Mechanical Vibrations: Measurement, Effects and Control*; Nova Science Publishers: New York, NY, USA, 2009.

11. Kaewunruen, S.; Remennikov, A. Dynamic Effect on Vibration Signatures of Cracks in Railway Prestressed Concrete Sleepers. *Adv. Mater. Res.* **2008**, *41–42*, 233–239. [CrossRef]

12. Ngamkhanong, C.; Kaewunruen, S.; Costa, B.J.A. State-of-the-Art Review of Railway Track Resilience Monitoring. *Infrastructures* **2018**, *3*, 3. [CrossRef]

13. Gamage, E.K.; Kaewunruen, S.; Remennikov, A.M.; Ishida, T. Toughness of Railroad Concrete Crossties with Holes and Web Openings. *Infrastructures* **2017**, *2*, 3. [CrossRef]

14. Kaewunruen, S.; You, R.; Ishida, M. Composites for Timber-Replacement Bearers in Railway Switches and Crossings. *Infrastructures* **2017**, *2*, 13. [CrossRef]

15. Kaewunruen, S.; Remennikov, A.M. Structural Safety of Railway Prestressed Concrete Sleepers. *Aust. J. Struct. Eng.* **2009**, *9*, 129–140. [CrossRef]

16. Griffin, D.W.P.; Mirza, O.; Kwok, K.; Kaewunruen, S. Finite Element Modelling of Modular Precast Composites for Railway Track Support Structure: A Battle to Save Sydney Harbour Bridge. *Aust. J. Struct. Eng.* **2015**, *16*, 150–168. [CrossRef]

17. SEKISUI Chemical Gmb, FFU Synthetic Railway Sleepers. Available online: https://www.sekisui-rail.com/en/ffu-synthetic-wood.html (accessed on 10 January 2020).

18. Gunther, K. FFU synthetic sleeper- Project in Europe. *Constr. Build. Mater.* **2015**, *92*, 42–50.

19. Takai, H.; Sato, Y.; Sato, K. Japanese Twenty Five years Experiences and Standardization of Synthetic Sleeper. Available online: http://www.railway-research.org/IMG/pdf/589.pdf (accessed on 15 January 2020).

20. NDT Resource Centre. Acoustic Emission (AE)—Introduction to Acoustic Emission Testing. Available online: https://www.nde-ed.org/AboutNDT/aboutndt.htm (accessed on 20 January 2020).

21. Graham, L.J.; Alers, G.A. Acoustic Emission in the Frequency Domain. In *Monitoring Structural Integrity by Acoustic Emission*; American Society for Testing and Materials: West Conshohocken, PA, USA, 1975; pp. 11–39.

22. Yilmazer, P. Structural Health Condition Monitoring of Rails Using Acoustic Emission Techniques. Master's Thesis, The University of Birmingham, Birmingham, UK, 2012.

23. Netravali, A.; Topoleski, L.; Sachse, W.; Phoenix, S. An acoustic emission technique for measuring fibre fragment length distributions in the single-fibre- composite test. *Compos. Sci. Technol.* **1989**, *35*, 13–29. [CrossRef]

24. Masayasu, O.; Masakatsu, U.; Takahisa, O.; Yuyama, S. Damage Assessment of Reinforced Concrete Beams Qualified by Acoustic Emission. *Struct. J.* **2002**, *99*, 411–417.

25. Nguyen, T.; Narintsoa, R.; Balayssaca, J. Characterization of damage in concrete beams under bending with Acoustic Emission Technique (AET). *Constr. Build. Mater.* **2018**, *187*, 487–500. [CrossRef]

26. Ramboll UK Ltd. Hammersmith Flyover—Phase 2 Refurbishment and Strengthening (HFO2). Available online: http://www.ramboll.co.uk/projects/ruk/hammersmith-flyover-phase-2#UHPFRC (accessed on 25 January 2020).

27. Webb, G.T.; Vardanega, P.J.; Fidler, P.R.A.; Middleton, C.R. Analysis of Structural Health Monitoring Data from Hammersmith Flyover. *J. Bridge Eng.* **2014**, *19*, 05014003. [CrossRef]

28. Janeliukstis, R.; Clark, A.; Papaelias, M.; Kaewunruen, S. Flexural cracking-induced acoustic emission peak frequency shift in railway prestressed concrete sleepers. *Eng. Struct.* **2019**, *178*, 493–505. [CrossRef]

29. Mccab, W.; Koerner, M.; Loard, J. An acoustic emission behavior of concrete laboratory specimens. *ACI J.* **1976**, *13*, 367–376.

30. Holcomb, D.J. General Theory of the Kaiser Effect. *J. Rock Mech. Min. Sci. Geomech. Abstr.* **1993**, *30*, 929–935. [CrossRef]

31. Grosse, C. Acoustic Emission (AE)—Kaiser Effect, NDT Encyclopedia. 2002. Available online: http://www.ndt.net/ndtaz/content.php?id=476 (accessed on 10 April 2020).

32. *BSI Standards Publication Railway Applications—Track—Concrete Sleepers and Bearers Part 2: Prestressed Monoblock Sleepers*; British Standards Institution (BSI): London, UK, 2016.

33. CALC RESOURSE. Calculation Tools & Engineering Resources. Deflections and Slopes of Simply Supported Beam. Available online: https://calcresource.com/statics-simple-beam.html (accessed on 25 April 2020).

34. Hibbeler, R.C. *Mechanics of Materials*, 7th ed.; Pearson—Prentice Hall: Englewood Cliffs, NJ, USA, 2007.

35. Michael, R.; Lindeburg, P.E. *PPI Mechanical Engineering Reference Manual for the PE Exam*, 13th ed.; (Hardcover) Comprehensive Reference Manual for the NCEES PE Exam; Professional Publications, Inc. (PPI): Belmont, CA, USA, 2013.

36. Richard, G. *Budynas. Shigley's Mechanical Engineering Design in SI Units*, 10th ed.; McGraw-Hill Education: New York, NY, USA, 2014.

37. Cai, Z. Modelling of Rail Track Dynamics and Wheel/Rail Interaction. Ph.D. Thesis, Department of Civil Engineering, Queen's University, Kingston, ON, Canada, 1992.

38. Grassie, S.L. Dynamic modelling of concrete railway sleepers. *J. Sound Vib.* **1995**, *187*, 799–813. [CrossRef]

39. Kaewunruen, S.; Remennikov, A.M. Sensitivity analysis of free vibration characteristics of an in situ railway concrete sleeper to variations of rail pad parameters. *J. Sound Vib.* **2006**, *298*, 453–461. [CrossRef]

40. Neilsen, J.C.O. Eigenfrequencies and eigenmodes of beam structures on an elastic foundation. *J. Sound Vib.* **1991**, *145*, 479–487. [CrossRef]

41. Remennikov, A.M.; Kaewunruen, S. Determination of prestressing force in railway concrete sleepers using dynamic relaxation technique. *J. Perform. Const. Fac.* **2015**, *29*, 04014134. [CrossRef]

42. Kaewunruen, S.; Lian, Q. Digital twin aided sustainability-based lifecycle management for railway turnout systems. *J. Clean. Prod.* **2019**, *228*, 1537–1551. [CrossRef]

43. Kaewunruen, S.; Remennikov, A.M. Field trials for dynamic characteristics of railway track and its components using impact excitation technique. *NDT&E Int.* **2007**, *40*, 510–519. [CrossRef]

44. Kaewunruen, S.; Ngamkhanong, C.; Ng, J. Influence of time-dependent material degradation on life cycle serviceability of interspersed railway tracks due to moving train loads. *Eng. Struct.* **2019**, *199*, 109625. [CrossRef]

45. Kaewunruen, S.; Sussman, J.M.; Matsumoto, A. Grand challenges in transportation and transit systems. *Front. Built Environ.* **2016**, *2*, 4. [CrossRef]

46. Janeliukstis, R.; Kaewunruen, S. A novel separation technique of flexural loading-induced acoustic emission sources in railway prestressed concrete sleepers. *IEEE Access.* **2019**, *7*, 51426–51440. [CrossRef]

47. Livermore Software Technology Corporation (LSTC). LS-dyna® Keyword User's Manual; Volume I, Version 971; 2007. Available online: http://lstc.com/pdf/ls-dyna_971_manual_k.pdf (accessed on 29 April 2020).